

Is organic photovoltaics promising for indoor applications?

Harrison K. H. Lee,^{1,a)} Zhe Li,^{1,a)} James R. Durrant,^{1,2} and Wing C. Tsoi^{1,b)}

¹*SPECIFIC, College of Engineering, Bay Campus, Swansea University, SAI 8EN Swansea, United Kingdom*

²*Department of Chemistry, Imperial College London, SW7 2AZ London, United Kingdom*

(Received 7 February 2016; accepted 8 June 2016; published online 20 June 2016)

This work utilizes organic photovoltaics (OPV) for indoor applications, such as powering small electronic devices or wireless connected Internet of Things. Three representative polymer-based OPV systems, namely, poly(3-hexylthiophene-2,5-diyl), poly[N-9'-heptadecanyl-2,7-carbazole-alt-5,5-(4',7'-di-2-thienyl-2',1',3'-benzothiadiazole)], and poly[[4,8-bis[(2-ethylhexyl)oxy]benzo[1,2-b:4,5-b']dithiophene-2,6-diyl][3-fluoro-2-[(2-ethylhexyl)carbonyl]thieno[3,4-b]thiophenediyl]], were selected as the donor materials in blend with fullerene derivatives for comparison under low light level condition using fluorescent lamps. PCDTBT based devices are found to be the best performing system, generating $13.9 \mu\text{W}/\text{cm}^2$ corresponding to 16.6% power conversion efficiency at 300 lx, although PTB7 based devices show the highest efficiency under one sun conditions. This high performance suggests that OPV is competitive to the other PV technologies under low light condition despite much lower performance under one sun condition. Different properties of these devices are studied to explain the competitive performance at low light level. A low energy consuming method for maximum power point tracking is introduced for the operation of the OPV devices. Finally, a $14 \text{ cm} \times 14 \text{ cm}$ OPV module with 100 cm^2 active area is demonstrated for real applications. These findings suggest that OPV, in particular, PCDTBT based devices, could be a promising candidate for indoor applications. *Published by AIP Publishing.*

[<http://dx.doi.org/10.1063/1.4954268>]

There is increasing interest in the development of photovoltaic (PV) technologies for low light applications which can be integrated with small scale consumer electronic devices or to power wireless connected Internet of Things (IoT), such as sensors, actuators, etc.^{1–5} The PV unit can provide power to the devices and thus prolong battery lifetime which reduces the frequency of costly and environmentally undesirable battery changing. Indoor PV refers to PVs used to harvest light energy from low light level environments such as homes and offices. Fluorescent lamps, at this moment, are perhaps still the most popular indoor lighting although light-emitting diodes (LED) are becoming more mature and competitive in the market. For indoor lighting, normally lux is used to indicate the light intensity level, accounting for human eye responsivity to different wavelengths; 200 lx is typical for living room environments and 300–500 lx for office environments.

Organic photovoltaic (OPV) cells have been fast developing in the past few years, especially solution-processed polymer:fullerene bulk-heterojunction system, with the power conversion efficiency (PCE) improving from less than 4% to higher than 11% under simulated one sun illumination.^{6–14} One major contribution to this performance enhancement is from the newly developed donor materials.^{8–14} As a result, researchers are changing their benchmark systems from poly(3-hexylthiophene-2,5-diyl) (P3HT), which was the most promising donor before 2009 to new donor materials, such as poly[N-9'-heptadecanyl-2,7-carbazole-alt-5,5-(4',7'-di-2-thienyl-2',1',3'-benzothiadiazole)] (PCDTBT) and poly[[4,8-bis[(2-

ethylhexyl)oxy]benzo[1,2-b:4,5-b']dithiophene-2,6-diyl][3-fluoro-2-[(2-ethylhexyl)carbonyl]thieno[3,4-b]thiophenediyl]] (PTB7). To date, studies on PCDTBT and PTB7 based devices have mostly focused on their performance under one sun conditions with their performance under low light levels relatively less understood. Recently, there has been some limited research on OPV blends, including P3HT, PTB7-Th based devices, as well as evaporated organic small molecule based devices for low light applications.^{15–17} However, a systematic comparison of the low light performance and operations of different benchmark OPV systems, as well as how that compares with typical solar conditions, is still lacking within the community.^{18–20}

In this work, we aim to study and compare the low light performance of OPV devices using three benchmarks polymers, P3HT, PCDTBT, and PTB7, to address their suitability for indoor applications. Unexpectedly, the highest power output and efficiency was obtained from PCDTBT based devices under indoor lighting, in contrast to that obtained under one sun conditions. We further carry out an in-depth characterization of the devices and summarize the criteria of OPV systems for indoor applications based on our findings. After this, an efficient large area OPV module based on PCDTBT is demonstrated for indoor applications. Connecting this to a circuit for real operation, high power transfer efficiency is obtained to power an electronic device or charge a battery.

P3HT was purchased from Rieke Metals. PCDTBT and PTB7 were purchased from 1-Material. The acceptor materials [6,6]-phenyl- C_{60} butyric acid methyl ester (PCBM) and [6,6]-phenyl C_{71} butyric acid methyl ester (PC₇₁BM) were obtained from Solenne BV. All materials were used as received. P3HT and PCBM with 1:0.8 mass ratio were

^{a)}H. K. H. Lee and Z. Li contributed equally to this work.

^{b)}Electronic mail: w.c.tsoi@swansea.ac.uk

dissolved in *o*-dichlorobenzene purchased from Aldrich with a total concentration of 36 mg/ml. PCDTBT and PC₇₁BM with 1:2 mass ratio were dissolved in chlorobenzene (CB) purchased from Aldrich with a total concentration of 18 mg/ml. PTB7 and PC₇₁BM with 1:1.5 mass ratio were dissolved in CB with 3 vol.% of 1,8-diiodooctane obtained from Tokyo Chemical Industry with a total concentration of 25 mg/ml. All the blend solutions were stirred on a 60 °C hotplate for at least 12 h. The blend solutions were spin-coated on poly(3,4-ethylenedioxythiophene)-poly(styrene-sulfonate) (PEDOT:PSS), Heraeus Clevios P VP AI 4083, coated indium-tin-oxide (ITO) substrates. The optimal spin speed for P3HT:PCBM, PCDTBT:PC₇₁BM, and PTB7:PC₇₁BM blends were 1000, 2000, and 2000 rpm, resulting in thicknesses of ~150, 70, and 110 nm, respectively. Then, 30 nm of calcium and 100 nm of aluminum were sequentially thermal evaporated onto the blend layers at 2×10^{-5} mbar forming devices with active area of 0.15 cm². For the PCDTBT:PC₇₁BM module, only the aluminum layer was evaporated as the cathode. P3HT:PCBM cells were post-annealed at 140 °C for 10 min. All devices were encapsulated by glass slides with the aid of epoxy before any measurement. Current density–voltage (*J*–*V*) characterizations were performed by a Keithley 2400 sourcemeter under AM1.5 G illumination, Newport 92193A-1000 solar simulator, or a series of fluorescent lamps with reflectors, Osram L18W/827. The lx level of the fluorescence lamps was measured by a luxmeter, LX-1330B. To mimic a real situation of a working area, 300 lx, a minimum light level of a typical office, was mainly used in this work to illuminate the OPV cells. The light intensity of the fluorescent lamps was calibrated by a Thorlabs PM100D power and energy meter equipped with a Thorlabs S401C high-sensitivity thermal sensor. To achieve different light intensity under one sun illumination, a series of optical density filters were employed.

Before comparing the low light performance, the performance of these OPV systems under one sun condition was first studied and the results are shown in Figure 1(a). From the *J*–*V* measurements, PTB7:PC₇₁BM device shows the highest *PCE* of 6.8% while PCDTBT:PC₇₁BM and P3HT:PCBM devices have *PCE* of 6.0% and 2.4%, respectively. These values agree well with the published results.^{6–11} Figure 1(b) shows the *J*–*V* curves obtained under fluorescent lamps with 300 lx illumination corresponding to light intensity of 83.6 μW/cm². The spectrum of the fluorescent lamps is shown in the inset of Figure 1(b). The maximum power output density, *P*_{max}, which is the product of short-circuit current density (*J*_{SC}), open-circuit voltage (*V*_{OC}), and fill factor (*FF*), are 4.8 μW/cm², 13.9 μW/cm², and 12.2 μW/cm² for P3HT:PCBM, PCDTBT:PC₇₁BM, and PTB7:PC₇₁BM corresponding to 5.8%, 16.6%, and 14.6% *PCE* at 300 lx, respectively. To date, the low light performance of PCDTBT:PC₇₁BM device is a record for polymer-based OPV in literature. Details of the performance are listed in Table I. In general, the *PCE* measured under 300 lx are significantly higher than that under one sun because the emission spectrum from the fluorescent lamps is mainly in the visible region, matching very well with the absorption of the polymers, while a considerable amount of infrared photons from the solar spectrum cannot be converted into electrons in these material systems.^{6–11}

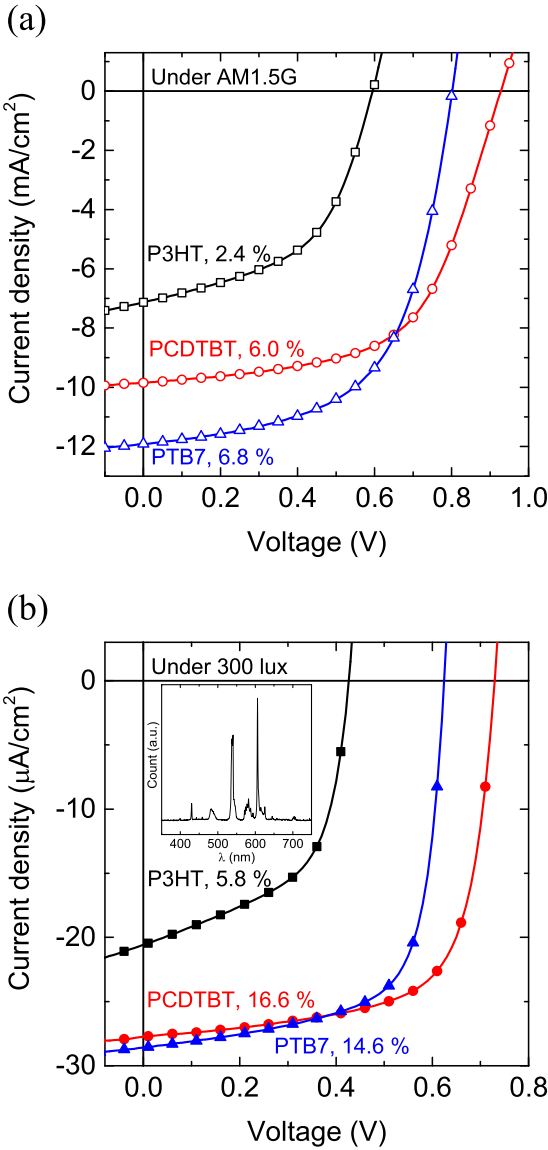


FIG. 1. *J*–*V* measurement of P3HT:PCBM (black square), PCDTBT:PC₇₁BM (red circle), and PTB7:PC₇₁BM (blue triangle) devices under (a) AM1.5 G condition with intensity of 82–90 mW/cm² and (b) 300 lx fluorescent lamps. The spectrum of 300 lx fluorescent lamps is shown in the inset.

Interestingly, the ranking of the performance is different from the performance under one sun. In both cases, P3HT:PCBM devices perform the worst. However, PCDTBT:PC₇₁BM devices performed better than PTB7:PC₇₁BM devices under low light condition, suggesting that the highest performing system under one sun is not necessarily the highest one under indoor condition.

TABLE I. Performance of P3HT:PCBM, PCDTBT:PC₇₁BM, and PTB7:PC₇₁BM OPV cells measured under 300 lx fluorescent lamps. The *PCE* measured under AM1.5 G are shown in the square brackets as reference.

	<i>J</i> _{SC} (μA/cm ²)	<i>V</i> _{OC} (V)	<i>FF</i> (%)	<i>P</i> _{max} (μW/cm ²)	<i>PCE</i> (%)
P3HT:PCBM	20.6	0.41	56.6	4.8	5.8 [2.4]
PCDTBT:PC ₇₁ BM	27.7	0.72	69.3	13.9	16.6 [6.0]
PTB7:PC ₇₁ BM	28.6	0.61	69.5	12.2	14.6 [6.8]

To understand what causes these differences, we compare their J_{SC} , V_{OC} , and FF under different light sources. First, J_{SC} can be correlated to the absorption of the donor material, which depends on the energy gap. Freunek *et al.* has calculated using the Shockley–Queisser analysis that the optimum bandgap energy required for harvesting the energy from fluorescent lamps or visible LED is 1.9 eV, whereas the optimum bandgap for AM1.5 G irradiation is smaller, 1.4 eV.¹⁹ The bandgap of PCDTBT is 1.9 eV, which matches well with this optimum value.⁸ On the other hand, PTB7 has a slightly smaller bandgap of 1.8 eV which can absorb more photons from the solar spectrum, but is a less ideal material for harvesting indoor light sources than PCDTBT.¹⁰ Second, V_{OC} is a light intensity dependent parameter.^{21–23} Generally, V_{OC} increases with the light intensity. From the equivalent circuit model and assuming high enough shunt resistance, R_{Sh} , the V_{OC} can be expressed as

$$V_{OC} \sim \frac{nkT}{e} \ln\left(\frac{I_{ph}}{I_0}\right), \quad (1)$$

where n is the ideality factor of the diode, k is the Boltzmann constant, T is the absolute temperature, e is the elementary charge, I_{ph} is the photocurrent, and I_0 is the saturation current of the diode. Quite often, in most OPV systems, I_{ph} is approximately linearly proportional to the incident light intensity.^{22,24–26} Thus, n is the primary factor that affects the proportionality between V_{OC} and logarithm of the light intensity if T is kept constant. For our devices, the J_{SC} is linearly proportional to the incident light intensity as shown in Figure S1 in good agreement with reports in the literature, which also supports the validity of extracting the ideality factor values using equation (1).^{22,24–27} Figure 2 shows the V_{OC} of the OPV cells studied herein at different light intensities under simulated solar conditions. In order to investigate light intensities for typical indoor PV applications, we performed our measurement starting from one sun level to three orders of magnitude lower intensity.^{15,28} In general, V_{OC} follows well with equation (1). The ideality factor of a diode, n , can

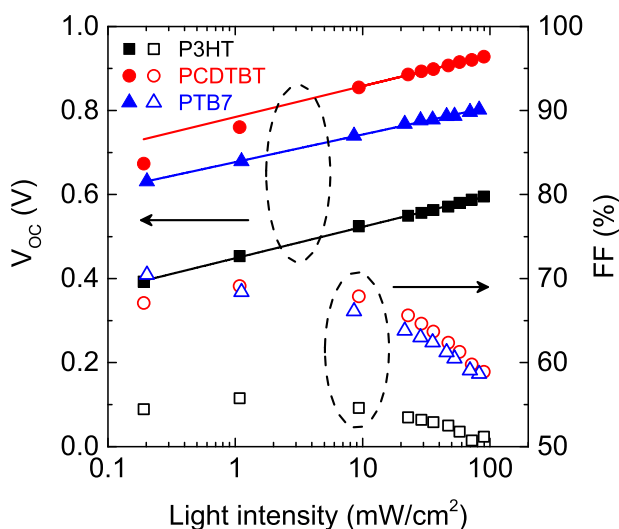


FIG. 2. V_{OC} (solid symbols) and FF (open symbols) of the three OPV devices at different light intensity of AM1.5 G. The two V_{OC} data points from the PCDTBT device at the lowest light intensity are not included in the fit.

be extracted from the slope of a linear fit. The extracted values of n are 1.25, 1.24, and 1.10 for the systems of P3HT:PCBM, PCDTBT:PC₇₁BM, and PTB7:PC₇₁BM, respectively. The values of n usually vary between 1 and 2 depending on how ideal the diode is, with $n = 1$ referring to an ideal diode.²⁹ We note that analysis using different evaluating methods may yield slightly different ideality factor values.^{22,23,30} Most OPV systems have ideality factors close to 1 if they are optimized, as observed for the devices herein.^{22,30} Besides having a low ideality factor, a high V_{OC} at one sun level could be more critical. The main reason of PCDTBT:PC₇₁BM devices outperforming PTB7:PC₇₁BM devices under low light condition is that the V_{OC} of PCDTBT:PC₇₁BM devices under one sun is higher than that of PTB7 by 0.13 V. With similar ideality factors, the percentage loss of the V_{OC} from one sun to 300 lx is smaller for a higher V_{OC} system like PCDTBT:PC₇₁BM. Here, we consider J_{SC} and V_{OC} separately. However, there is usually a trade-off between J_{SC} and V_{OC} in OPV systems as they are simultaneously affected by the energy levels of the donor and acceptor materials.³¹ Mori *et al.* performed simulations using different values of highest occupied molecular orbital and lowest unoccupied molecular orbital for organic donor material and fixed the energy levels of the PC₇₁BM acceptor to guide chemists to design new donor materials for low light applications.¹⁷ Third, for all the systems, the FF increases with decreasing light intensity to a level which is suitable for low light applications as shown in Figure 2. In particular, the FF of the PCDTBT:PC₇₁BM device rises from 59% at 0.9 sun to 69% at 0.01 sun. The other two systems also show similar trends. For an indoor light level, 300 lx, the FF remains at a high value for each of the system: 57% for P3HT:PCBM and close to 70% for both PCDTBT:PC₇₁BM and PTB7:PC₇₁BM. These results are in agreement with earlier reports.^{15,17,28} To achieve a high FF under low light condition, a large shunt resistance is critical unlike for one sun applications in which a small series resistance (R_S) is necessary. Steim *et al.* showed that a shunt resistance of at least 85 kΩ cm² is required for indoor applications.¹⁵ For the devices in this study, the shunt resistance extracted from the J - V curves under 300 lx are 76, 228, and 229 kΩ cm² for P3HT:PCBM, PCDTBT:PC₇₁BM, and PTB7:PC₇₁BM devices, respectively, which is well above the suggested values except the P3HT:PC₇₁BM devices. The corresponding series resistances of these devices are available in the Table S1 of Ref. 27.

The maximum power density generation at different light levels is useful for different indoor use purposes. Figure 3 shows the P_{max} of the OPV devices from 100 lx to 1000 lx. This range covers most of the light levels for indoor environments. All the P_{max} behave quite linearly in this illumination range although individual parameters such as V_{OC} and FF vary differently with the illuminance. From this plot, for a known light level and power required, the active area needed for a particular application can be estimated.

In real applications, devices should operate at their maximum power point (MPP) to maximize the efficiency, in which the corresponding current and voltage are defined as I_{max} and V_{max} . Typically, the perturb-and-observe method is used to track the MPP of outdoor PV.^{32,33} However, this

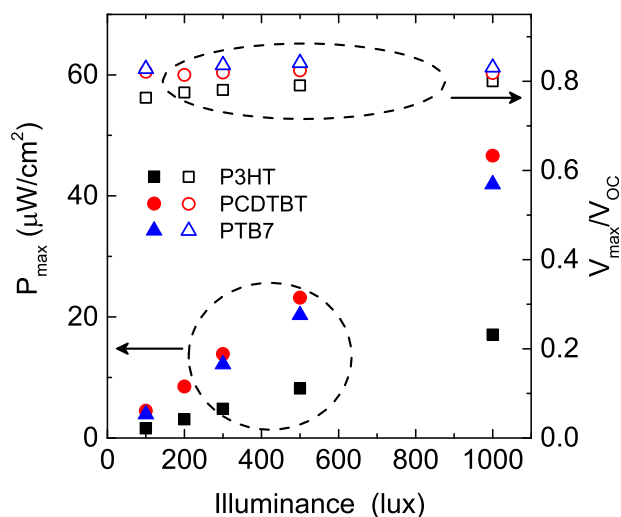


FIG. 3. Maximum power output density, P_{\max} , (solid symbols) and V_{\max} to V_{OC} ratio (open symbols) of 3 OPV devices at different illumination levels of fluorescent lamps.

method requires relatively high power to operate compared with the power generated from indoor PV. To minimize the power consumption, a simpler fractional-voltage method can be employed for indoor PV.^{34,35} This method requires a stable ratio of V_{\max} to V_{OC} so that the ratio can be preset to the electronic circuit to maintain high power output. Figure 3 shows the ratios of V_{\max} to V_{OC} for the OPV devices at different illuminances. For these OPV devices, the ratios are stable in this illumination range, especially for PCDTBT:PC₇₁BM and PTB7:PC₇₁BM having high values of 0.81–0.82 and 0.83–0.84, respectively.

Our PCDTBT:PC₇₁BM OPV cells perform the best among the other OPV devices at low light level environment generating $13.9 \mu\text{W}/\text{cm}^2$ under 300 lx. We now address whether this is competitive compared with other PV technologies. Using 300 lx as a reference, we compare the performance with other relatively mature PV technologies published recently. Teran *et al.* reported the performance of gallium arsenide and polycrystalline silicon cells at 300 lx showing P_{\max} of around $\sim 12.5 \mu\text{W}/\text{cm}^2$ and $\sim 2.5 \mu\text{W}/\text{cm}^2$, respectively.³⁶ De Rossi *et al.* tested their customized dye-sensitized solar cell (DSC) and some commercially available amorphous silicon (a-Si) cells. The highest P_{\max} at 300 lx are $\sim 12.5 \mu\text{W}/\text{cm}^2$ for their DSC and $\sim 9.1 \mu\text{W}/\text{cm}^2$ for the best a-Si cell.³⁷ Our findings show that OPV cells using suitable materials can compete with these developed PV technologies with potentially much lower cost especially compared with those inorganic PV.

Upscaling of OPV cell has been a concern for outdoor applications due to the high series resistance from large area modules causing lower FF .^{38,39} However, for indoor applications, series resistance is less critical. Instead shunt resistance is more critical to the device performance.¹⁵ As a demonstration, we fabricated an 8-pixel module by spin-coating PCDTBT:PC₇₁BM blend solution on a substrate of $14 \text{ cm} \times 14 \text{ cm}$ with an active area of 100 cm^2 as shown in Figure 4. The module generates I_{SC} of $314 \mu\text{A}$, V_{OC} of 4.87 V , and FF of 61.2% under 300 lx. Due to the potential inhomogeneity issues of the simulated solar illumination

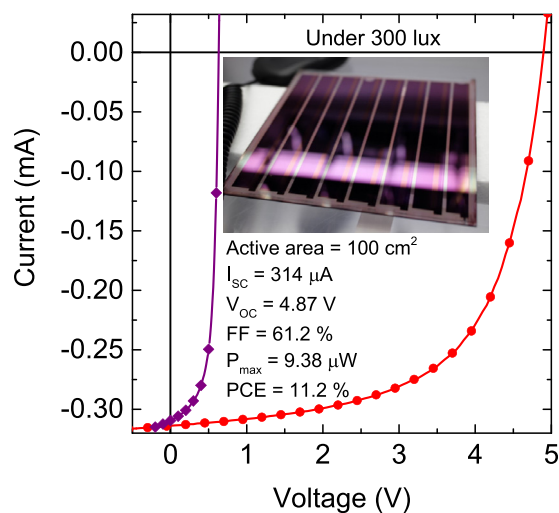


FIG. 4. I - V curves of 8 pixels connected in series (red circle) and a pixel (purple diamond), respectively, of the PCDTBT:PC₇₁BM module. The module has a dimension of $14 \text{ cm} \times 14 \text{ cm}$ with a total active area of 100 cm^2 . A photo of the module is shown in the inset.

over a large area of our OPV module, an estimated PCE of less than 2% is obtained under one sun. By evaluating a pixel with an area of 12.5 cm^2 in the module as shown in Figure 4, the R_{Sh} and R_{S} extracted are $383 \text{ k}\Omega \text{ cm}^2$ and $1058 \Omega \text{ cm}^2$, respectively. The R_{Sh} is even higher than that of the small area devices which is probably due to an averagely thicker active layer prepared by spin coating a large film. The series resistance is increased compared with that of the small area devices due to longer ITO pathway throughout the 8-pixel. Although the active area is much bigger than the small area device, the FF does not drop much. The maximum power extracted is $938 \mu\text{W}$ corresponding to 11.2% PCE which is currently the best OPV module demonstrated for indoor applications. The V_{\max} to V_{OC} ratios of the module are obtained at different illumination levels, as shown in Figure S2.²⁷ The values only vary between 0.75 and 0.77 from less than 100 lx to over 2000 lx, similar to that of small area devices. The module was then tested with a circuit with fractional-voltage method to maintain high power output from the module. Only less than 5% of the power generated by the module was dissipated to the circuit.

To conclude, we compared the performance of three generations of polymer-based devices blended with fullerene, P3HT, PCDTBT, and PTB7, under low light environment. PCDTBT:PC₇₁BM was found to be not only the best performing among them generating P_{\max} of $13.9 \mu\text{W}/\text{cm}^2$ with PCE of 16.6% under 300 lx but also the highest polymer-based OPV for indoor applications among the reported literatures. Surprisingly, the PCDTBT:PC₇₁BM devices outperform the PTB7:PC₇₁BM devices under low light, although PTB7:PC₇₁BM shows a higher PCE under one sun. It suggests that we should not just look at the PCE under one sun to select a system for indoor applications. For PCDTBT:PC₇₁BM devices, the optimum energy gap of PCDTBT, high V_{OC} under one sun, and low ideality factor result in high device performance under low light which can compete with many other mature PV technologies. With the stable V_{\max} to V_{OC} ratio of the OPV devices, a less power

consuming MPP tracking method, fractional-voltage method, is introduced for the operation of OPV devices. A large PCDTBT:PC₇₁BM module is demonstrated with good performance showing that OPV is suitable and competitive for practical indoor applications. This work also provides a more representative low light performance for polymer-based OPV to compare with different other PV technologies.

We are very grateful to Sêr Cymru funding from the Welsh Assembly Government, and further financial support from CEC EERA Cheetah Project (609788). We thank P. Shakya Tuladhar and S. Villarroja-Lidon for the experimental and technical supports, respectively. We acknowledge B. Bradley, A. Duller from Afterthought Software, and H. Davies from Solar Press for the collaboration.

- ¹J. Matiko, N. Grabham, S. Beeby, and M. Tudor, *Meas. Sci. Technol.* **25**, 012002 (2014).
- ²A. Nasiri, S. A. Zabalawi, and G. Mandic, *IEEE Trans. Ind. Electron.* **56**, 4502 (2009).
- ³M. Gorlatova, P. Kinget, I. Kymissis, D. Rubenstein, X. Wang, and G. Zussman, *IEEE Wireless Commun.* **17**, 18 (2010).
- ⁴K. Niotaki, A. Collado, A. Georgiadis, K. Sangkil, and M. M. Tentzeris, *Proc IEEE* **102**, 1712 (2014).
- ⁵H. Jayakumar, K. Lee, W. S. Lee, A. Raha, Y. Kim, and V. Raghunathan, "Powering the internet of things," in *Proceedings of the 2014 International Symposium on Low Power Electronics and Design, La Jolla, USA, 11–13 August 2014* (2014), pp. 375–380.
- ⁶G. Dennler, M. C. Scharber, and C. J. Brabec, *Adv. Mater.* **21**, 1323 (2009).
- ⁷X. Yang and A. Uddin, *Renewable Sustainable Energy Rev.* **30**, 324 (2014).
- ⁸S. H. Park, A. Roy, S. Beaupré, S. Cho, N. Coates, J. S. Moon, D. Moses, M. Leclerc, K. Lee, and A. J. Heeger, *Nat. Photonics* **3**, 297 (2009).
- ⁹S. Beaupré and M. Leclerc, *J. Mater. Chem. A* **1**, 11097 (2013).
- ¹⁰Y. Liang, Z. Xu, J. Xia, S.-T. Tsai, Y. Wu, G. Li, C. Ray, and L. Yu, *Adv. Mater.* **22**, E135 (2010).
- ¹¹Z. He, C. Zhong, S. Su, M. Xu, H. Wu, and Y. Cao, *Nat. Photonics* **6**, 591 (2012).
- ¹²S.-H. Liao, H.-J. Jhuo, Y.-S. Cheng, and S.-A. Chen, *Adv. Mater.* **25**, 4766 (2013).
- ¹³Z. He, B. Xiao, F. Liu, H. Wu, Y. Yang, S. Xiao, C. Wang, T. P. Russell, and Y. Cao, *Nat. Photonics* **9**, 174 (2015).
- ¹⁴Y. Liu, J. Zhao, Z. Li, C. Mu, W. Ma, H. Hu, K. Jiang, H. Lin, H. Ade, and H. Yan, *Nat. Commun.* **5**, 5293 (2014).
- ¹⁵R. Steim, T. Ameri, P. Schilinsky, C. Waldauf, G. Dennler, M. Scharber, and C. J. Brabec, *Sol. Energy Mater. Sol. Cells* **95**, 3256 (2011).
- ¹⁶K. Cnops, E. Voroshazi, C. Hart de Ruijter, P. Heremans, and D. Cheyns, in *Proceedings of the 40th IEEE Photovoltaic Specialist Conference* (2014), p. 143.
- ¹⁷S. Mori, T. Gotanda, Y. Nakano, M. Saito, K. Todor, and M. Hosoya, *Jpn. J. Appl. Phys., Part 1* **54**, 071602 (2015).
- ¹⁸N. Sridhar and D. Freeman, "A study of dye sensitized solar cells under indoor and low level outdoor lighting: comparison to organic and inorganic thin film solar cells and methods to address maximum power point tracking," in *Proceedings of the 26th European Photovoltaic Solar Energy Conference and Exhibition, Hamburg, Germany, 5–9 September 2011* (2011), pp. 232–236.
- ¹⁹M. Freunek, M. Freunek, and L. M. Reindl, *IEEE J. Photovoltaics* **3**, 59 (2013).
- ²⁰B. Minnaert and P. Veelaert, *Energies* **7**, 1500 (2014).
- ²¹L. J. A. Koster, V. D. Mihailetschi, R. Ramaker, and P. W. M. Blom, *Appl. Phys. Lett.* **86**, 123509 (2005).
- ²²S. R. Cowan, A. Roy, and A. J. Heeger, *Phys. Rev. B* **82**, 245207 (2010).
- ²³T. Kirchartz, F. Deledalle, P. S. Tuladhar, J. R. Durrant, and J. Nelson, *J. Phys. Chem. Lett.* **4**, 2371 (2013).
- ²⁴L. J. A. Koster, V. D. Mihailetschi, H. Xie, and P. W. M. Blom, *Appl. Phys. Lett.* **87**, 203502 (2005).
- ²⁵Z. Li, G. Lakhwani, N. C. Greenham, and C. R. McNeill, *J. Appl. Phys.* **114**, 034502 (2013).
- ²⁶A. K. K. Kyaw, D. H. Wang, V. Gupta, W. L. Leong, L. Ke, G. C. Bazan, and A. J. Heeger, *ACS Nano* **7**, 4569 (2013).
- ²⁷See supplementary material at <http://dx.doi.org/10.1063/1.4954268> for additional device characterization.
- ²⁸K. Tada, *Org. Electron.* **30**, 289 (2016).
- ²⁹S. M. Sze, *Semiconductor Devices*, 2nd ed. (John Wiley & Sons, New York, 2002).
- ³⁰P. de Bruyn, A. H. P. van Rest, G. A. H. Wetzelaer, D. M. de Leeuw, and P. W. M. Blom, *Phys. Rev. Lett.* **111**, 186801 (2013).
- ³¹E. T. Hoke, K. Vandewal, J. A. Bartelt, W. R. Mateker, J. D. Douglas, R. Noriega, K. R. Graham, J. M. J. Fréchet, A. Salleo, and M. D. McGehee, *Adv. Energy Mater.* **3**, 220 (2013).
- ³²D. P. Hohm and M. E. Ropp, "Comparative study of maximum power point tracking algorithms using an experimental, programmable, maximum power point tracking test bed," in *Proceedings of the IEEE 28th Photovoltaic Specialists Conference, Brookings, USA, 15–22 September 2000* (2000), pp. 1699–1702.
- ³³N. Femia, G. Petrone, G. Spagnuolo, and M. Vitelli, *IEEE Trans. Power Electron.* **20**, 963 (2005).
- ³⁴W. S. Wang, T. O'Donnell, N. Wang, M. Hayes, B. O'Flynn, and C. O'Mathuna, *ACM J. Emerging Technol.* **6**, 6 (2010).
- ³⁵I. Mathews, G. Kelly, P. J. King, and R. Frizzell, "GaAs solar cells for indoor light harvesting," in *Proceedings of the IEEE 40th Photovoltaic Specialist Conference, Denver, USA, 8–13 June 2014* (2014), pp. 510–513.
- ³⁶A. S. Teran, J. Wong, W. Lim, G. Kim, Y. Lee, D. Blaauw, and J. D. Phillips, *IEEE Trans. Electron Devices* **62**, 2170 (2015).
- ³⁷F. De Rossi, T. Pontecorvo, and T. M. Brown, *Appl. Energy* **156**, 413 (2015).
- ³⁸R. Tipnis, J. Bernkopf, S. Jia, J. Krieg, S. Li, M. Storch, and D. Laird, *Sol. Energy Mater. Sol. Cells* **93**, 442 (2009).
- ³⁹H.-K. Lyu, J. H. Sim, S.-H. Woo, K. P. Kim, J.-K. Shin, and Y. S. Han, *Sol. Energy Mater. Sol. Cells* **95**, 2380 (2011).